Transverse momentum correlations between particle-particle pairs as a probe of effective emitter mass : 40Ar+natAg (E/A=7, 17, 27, and 34 MeV)

T. Ethvignot, N.N. Ajitanand, J.M. Alexander, A. Elmaani, C.J. Gelderloos, P. Desesquelles, H. Elhage, A. Giorni, D. Heuer, S. Kox, et al.

Transverse momentum correlations between particle-particle pairs as a probe of effective emitter mass: $^{40}Ar + ^{nat}Ag$ ($E/A = 7$, 17, 27, and 34 MeV)

T. Ethvignot,[1,2,*] N. N. Ajitanand,[1] J. M. Alexander,[1] A. Elmaani,[1,†] C. J. Gelderloos,[1] P. Désesquelles,[2] H. Elhage,[2] A. Giorni,[2] D. Heuer,[2] S. Kox,[2] A. Lleres,[2] F. Merchez,[2] C. Morand,[2] D. Rebreyend,[2] P. Stassi,[2] J. B. Viano,[2] F. Benrachi,[3] B. Chambon,[3] B. Cheynis,[3] D. Drain,[3] and C. Pastor[3]

[1]*State University of New York at Stony Brook, Stony Brook, New York 11794*

[2]*Institut des Sciences Nucléaires de Grenoble, Institut National de Physique Nucléaire et de Physique des Particules–Centre National de la Recherche Scientifique/Université Joseph Fourier de Grenoble 53, Avenue des Martyrs, 38026, Grenoble CEDEX, France*

[3]*Institut de Physique Nucléaire de Lyon, Institut National de Physique Nucléaire et de Physique des Particules–Centre National de la Recherche Scientifique/Université Claude Bernard 43, Boulevard du 11 Novembre 1918, Villeurbanne CEDEX, France*

(Received 3 September 1992; revised manuscript received 23 February 1993)

Average transverse momenta have been carefully measured for α-particle pairs at laboratory angles of 21°, 31°, 47°, and 67°. They exhibit small but distinct shifts for different relative azimuthal angles $\Delta\varphi$. Detection on the same side of the beam ($\Delta\varphi \approx 24°$) yields a smaller average tranverse momentum or energy than on the opposite side ($\Delta\varphi \approx 168°$). For α-α pairs detected at $\approx 67°$ to the beam these small shifts are analyzed with a recoil model to extract the average emitter mass for the first α particle from the coincident pairs. The results are $A = 130 \pm 10$ to 115 ± 10 for reactions of $^{107,109}Ag$ with ^{40}Ar for $7A$ and $34A$ MeV, respectively. The particle pairs emitted at 21° are produced from more complex source mixtures. There is evidence from p-Li and α-Li pairs that Li fragments are emitted after protons or α particles in $\approx \frac{1}{2}$ of the events. The overall pattern is consistent with incomplete fusion leading to the formation of a hot, essentially thermalized composite nucleus and its associated statistical decay.

PACS number(s): 25.70.−z

Heavy ion reactions at near-barrier energies (i.e., $< 10A$ MeV) are broadly classified as quasielastic, deeply inelastic, or (essentially) complete fusion. The most peripheral quasielastic collisions involve very little energy dissipation in contrast to the more central fusion collisions characterized by essentially complete energy dissipation into a composite nucleus. As the incident energy is increased above $\approx 10A$ MeV, the more central collisions become dominated by incomplete fusion reactions, which continue to involve large energy dissipation into a composite nucleus but also a substantial loss of mass due to the ejection on impact of a spray of nucleons, α particles, etc. (See, for example, Ref. [1].) For even higher energies one imagines that an explosive nuclear fireball is created in a dense collision region of projectile-target overlap while remnants of the projectile and target may escape as excited nuclei that are sometimes called spectators [2].

Accelerators of intermediate energy heavy ions ($> 10A$ MeV) have been available for a relatively short time so one does not yet have a clear picture of the evolution between these reaction classes. In this work we study the reaction $^{40}Ar + ^{nat}Ag$ from the near-barrier energy domain of $7A$ MeV to the near-Fermi-energy domain of $34A$ MeV. Substantial changes in the reaction characteristics have been predicted for this wide span of incident energies [2,3]. For $7A$ MeV one knows that the central collisions are dominated by essentially complete fusion followed by evaporation. However, the increase of incident energy to $34A$ MeV could conceivably vaporize the system into nucleons, α particles, etc. Hence we wish to ask if composite nuclear systems can accept the highly dissipative impacts without loss of their capability for collective recoil and rotational motions. Our probe is the coincident detection of ejectile pairs, which, in this study, we examine carefully for the signs of collective recoil by an emission source. Then we use the magnitude of this recoil to characterize the mass of the source. In closely related work with the same detection array [4] we have used the magnitudes of azimuthal angular anisotropies to characterize the rotational motions of the source [5].

Experimental data were obtained by the AMPHORA multidetector array [4] with ^{40}Ar beams of $7A$, $17A$, $27A$, and $34A$ MeV from the SARA facility at Grenoble. Of the several targets used, we concentrate here on the reactions with ^{nat}Ag. Results from this experiment have been presented at various conferences and some have been published already [5–7]; more are still being ana-

*Present address: Centre d'Etudes de Bruyères-le-Châtel, B.P. No. 12, 91680 Bruyères-le-Châtel, France.

†Present address: Nuclear Physics Laboratory, GL-10, University of Washington, Seattle, WA 98195.

lyzed. AMPHORA consists of 140 CsI detectors ($\approx 85\%$ of 4π), 48 of which are located in a forward wall extending from $\approx 2°$ to 15°, and 92 of which are arranged in "crown rings" with cylindrical symmetry around the beam axis. The isotopes of ^{1,2,3}H and ^{3,4}He are uniquely identified along with groups for $Z=3$ (Li) and $Z>3$ (heavy fragments). In an earlier paper we presented results on polar angular distributions for inclusive particles and azimuthal angular correlations for particle pairs [5]. Here we study the average transverse momenta of pairs of particles [8], especially α-α pairs. We search for small shifts in the average transverse momentum as a function of relative azimuthal angle $\Delta\varphi$ between the particles; such shifts can lead to a measure of the mass of the emission source for these particles.

Figure 1 shows the (polar) angular distributions for single α particles and for α-α pairs (detected in the same ring). These cross sections have been transformed into the moving frame of the struck nucleus after incomplete fusion. The average velocity of this moving system has been measured for $7A$ and $17A$ MeV to correspond to linear momentum transfers (LMT) of $\approx 100\%$ and 85%, respectively [9,10]. Systematic studies of similar reaction systems [11] allow for LMT estimates of $\approx 80\%$ and 70% for E/A of 27 and 34 MeV. The major feature of these angular distributions is the nearly isotropic emission in the backward hemisphere for each bombarding energy. It was already well known that composite nucleus formation and decay is the dominant source of particle emission for E/A of 7 and 17 MeV [9,12], but the apparent continuation of the dominance of this mechanism to $34A$ MeV has come to us as a surprise [5].

From Fig. 1 we note that the isotropic region extends forward to $\approx 90°$ (or ring 4 at $\theta_{lab} \approx 67°$ in AMPHORA), and that a strong forward peak dominates at $\approx 30°$ (or ring 7 in AMPHORA at $\theta_{lab} \approx 21°$). Hence we decided to look in detail at the properties of particle pairs detected over this angular region (i.e., rings 4–7 in AMPHORA, each with 15 detectors subtending 24° in azimuthal angle). The angular distributions in Fig. 1 suggest mainly prethermalization emission at the small angles and post thermalization emission at the large angle ($\theta_{lab}=67°, \theta_{c.m.} \approx 90°$).

The H-He multiplicity distributions are shown in Fig. 2 as triggered by α-α pairs detected in these four rings. For each incident ^{40}Ar energy, these multiplicity distributions follow the same pattern. If the α-α trigger pair is found at $\approx 67°$, then the H-He multiplicity distribution is nearly Gaussian with a large mean value, which has been shown to be typical of the central-collision group [6]. If the α-α trigger pair is found at more forward angles (particularly 21°), then the average H-He multiplicity is smaller and the distribution has a tail of low-multiplicity events along with the peak at high multiplicity. Apparently a mixture of reaction classes is contributing to the α-α pairs at small angles and especially for $\theta_{lab} \approx 21°$ [6].

Further evidence for this conclusion is provided in Fig. 3 where we show α-particle energy spectra detected at two separate angles and triggered with three separate gates on H-He multiplicity. The α spectra from ring 4 ($56° < \theta < 78°$) are Maxwellian and evaporationlike. They have only a slight dependence on the multiplicity gate used. By contrast the α spectra from ring 7 ($15° < \theta < 25°$) are more complex with strong dependence on the multiplicity gate. These results seem to indicate one dominant thermalized emitter group for the α-α

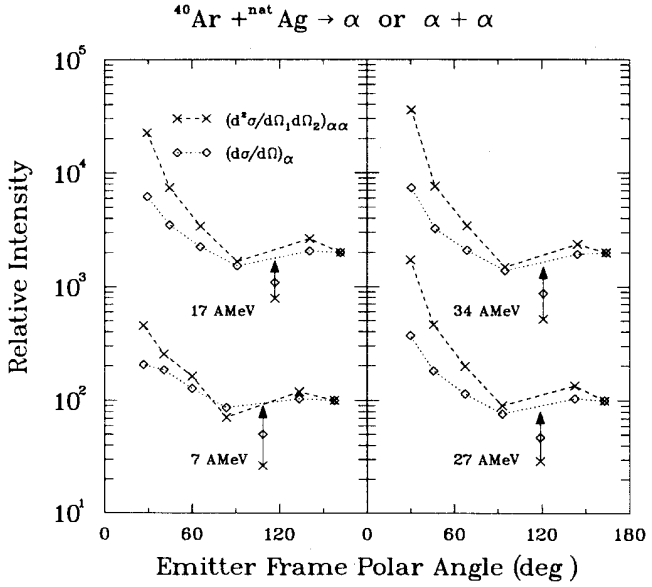

FIG. 1. Angular distributions (arbitrary units) for inclusive α particles and for α-α pairs in the emitter frame. The emitter-frame velocity is taken from systematic studies (Refs. [9–11]) of linear momentum transfer (100%, 85%, 80%, and 70% for $7A$, $17A$, $27A$, and $34A$ MeV, respectively).

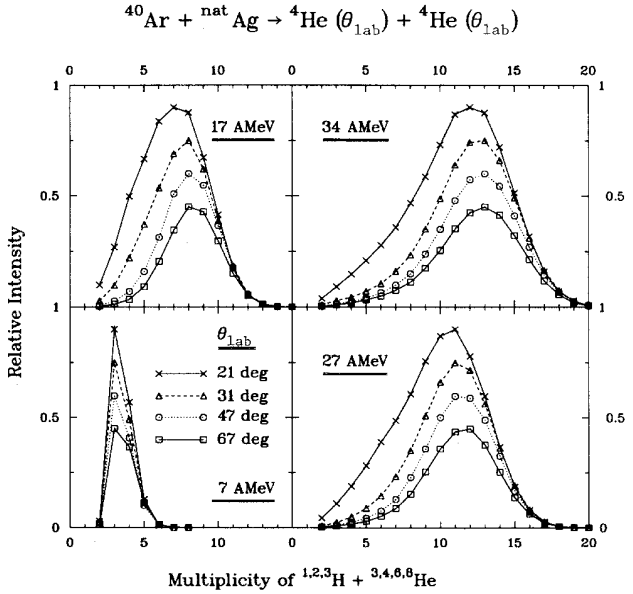

FIG. 2. H-He multiplicity distributions (arbitrary normalizations) triggered by an α-α pair at the indicated angle. No efficiency corrections have been made; a rough correction can be made by multiplying each abscissa value by ≈ 1.5 (Ref. [5]).

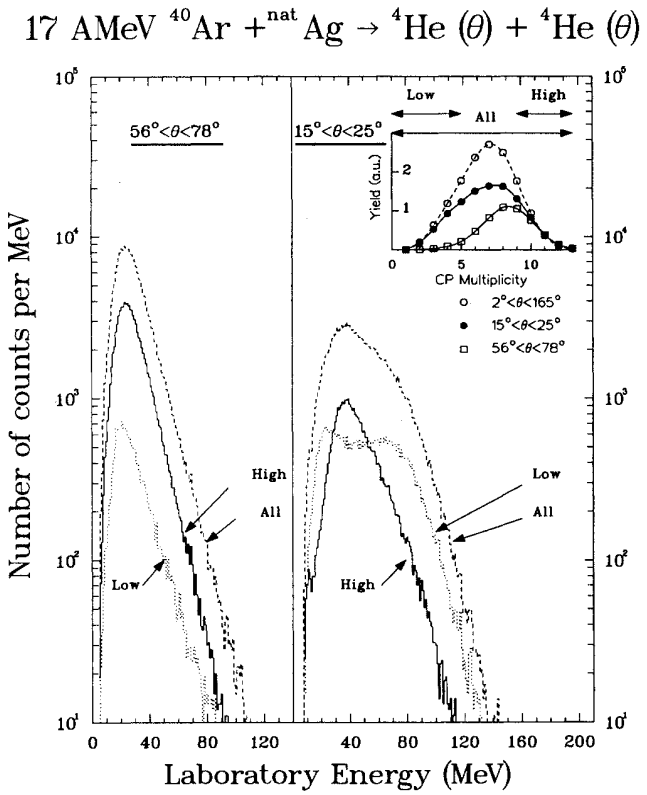

FIG. 3. ^{4}He energy distributions for detection in pairs at the two indicated angles. The inset shows exclusive charged particle (CP) multiplicity distributions as observed in all of AMPHORA in coincidence with α pairs detected in the indicated angular zones. The three ^{4}He spectra in each box were gated by the multiplicity conditions labeled All, High, or Low as delineated in the inset.

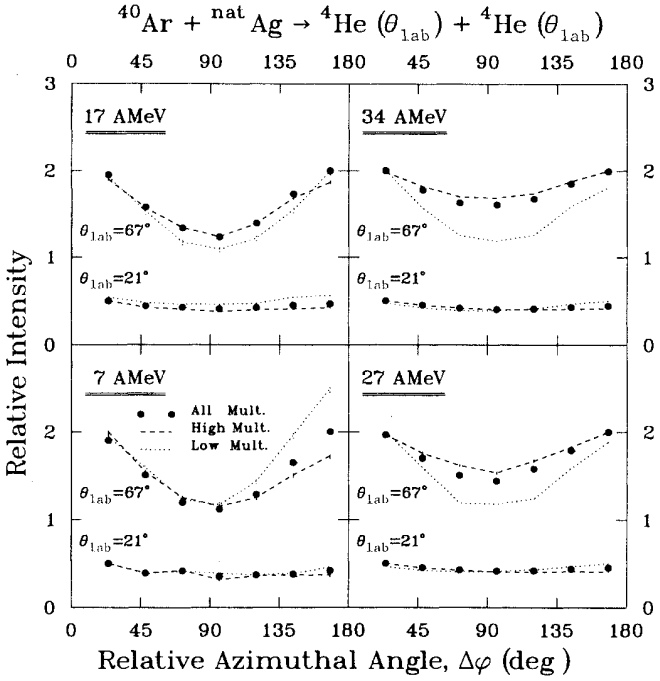

FIG. 4. Azimuthal angular correlations (θ and $\Delta\varphi$ in the laboratory frame) for α-α pairs for the cases indicated. Gating conditions labeled All are for all LCP multiplicities. Gating conditions labeled Low are for LCP ≤ 3, LCP ≤ 5, LCP ≤ 7, and LCP ≤ 7 for respectively 7 A, 17 A, 27 A, and 34 A MeV. Similarly gating conditions labeled High are for LCP ≥ 4, LCP ≥ 9, LCP ≥ 12, and LCP ≥ 12. (See Figs. 2 and 3.)

pairs at $\theta \approx 67°$, but at least two emission sources or mechanisms for the α-α pairs at $\theta \approx 21°$.

Figure 4 shows azimuthal angular correlations for α-α pairs detected at the same two angles and triggered with the same three gates on H-He multiplicity. The correlations are almost flat for $\theta \approx 21°$. Let us focus here on the more interesting correlations for $\theta_{lab} = 67°$ with gates on high or all multiplicity; they have essentially the same shapes with distinct anisotropies that favor $\Delta\varphi = 0°$ and 180° but are almost symmetric about $\Delta\varphi = 90°$ [5]. This is the behavior expected for a hot spinning nuclear source [13]. In Ref. [6] we showed that the α-α pairs at $\theta \approx 67°$ come from a central-collision group characterized by entrance channel spins of zero to at least $150\hbar$. In Refs. [5] and [13] we showed that the statistical model can account for these distinct anisotropies at 67° if the maximum emitter spin is $\approx (100-130)\hbar$.

The statistical model framework used [5,12,13] is based on the notion of extensive thermalization or collisional energy mixing in a composite nuclear system. The mean lifetime of such a composite system (excited to 3–5 MeV per nucleon) could be very short indeed, e.g., of order 10^{-22} s [12]; therefore, its capacity to act collectivity in momentum and energy sharing is of great interest [2,3].

To explore this collectivity of momentum sharing, we search for a measure of the average mass of these short-lived transient nuclear systems.

An obvious way to try to determine the effective mass of this emitter group is through its recoil kicks due to particle ejection [8]. In the simplest scenario one can imagine that one α particle gives a recoil to the residual nucleus, which then emits a second α particle. Figure 5

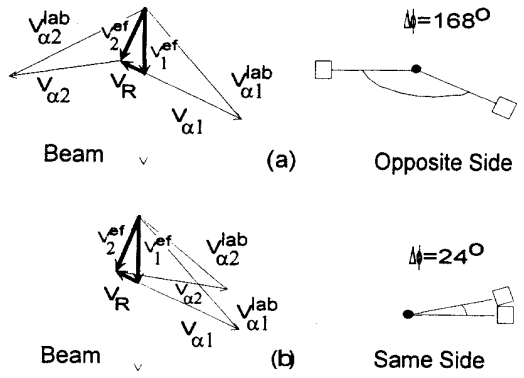

FIG. 5. Schematic vector diagram for successive emission of two α particles (subscripts 1 and 2) for two detector configurations: (a) opposite side or $\Delta\varphi \approx 168°$; (b) same side or $\Delta\varphi \approx 24°$. Subscripts and superscripts for each velocity V are α for an α particle, ef for an emitter frame, R for the nuclear recoil due to the first α emission.

shows a vector diagram for the successive ejection of two such α particles in two different configurations: (a) on almost opposite sides so that they hit detectors with $\Delta\varphi \approx 180°$ and (b) on almost the same side so that they hit detectors with $\Delta\varphi \approx 24°$. In the opposite (same) side configuration it is clear that the larger the recoil velocity V_R, the larger (smaller) the sum of the transverse velocities of the two α particles. Although this schematic diagram has been drawn for equal α velocities in the emitter frame ($V_{\alpha 1}$ and $V_{\alpha 2}$), the point still holds for any other choices. Therefore, the magnitude of the average transverse momentum (or energy) shift between α-α pairs on the same vs opposite sides can give a means to sense the average recoil velocity and deduce the average emitter mass. In other words, momentum conservation provides the relationship between the average recoil mass and the average change in transverse α momentum $\Delta[\langle P_{\perp 1}\rangle + \langle P_{\perp 2}\rangle]/2$ for the opposite vs same side configurations. The major assumption for this approach is intrinsic right-left symmetry for particle emission in the emitter frame; the azimuthal distributions in Fig. 4 support this assumption for $\theta = 67°$. It is this condition of right-left emission symmetry that generates a nil effect, *on average*, for all the other particles in the event cascade. We have verified this expectation by Monte Carlo reaction simulations, some of which are discussed below.

In Fig. 6 we show the observed shifts in transverse momentum (Δ) for α-α pairs detected in crown rings centered at 21°, 31°, 47°, 67°. These shifts for 67° are only ≈ 10 MeV/c or $\approx 2.5\%$ in momentum and $\approx 5\%$ in energy. Nevertheless, they can be measured reliably if one gives special attention to experimental details. The major point is that each detector is used to the same extent in both the same and opposite side measurements; one cancels imperfections by averaging over the same detector responses in the same experimental run.

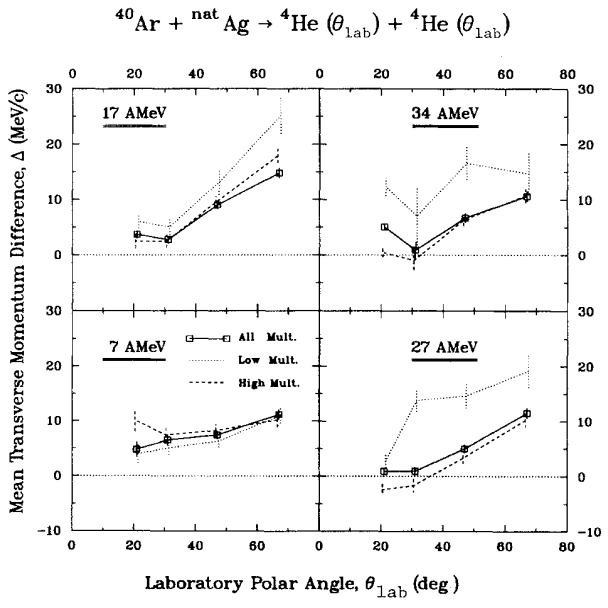

FIG. 6. Mean transverse momentum difference $\Delta = \Delta[\langle p_{\perp 1}\rangle + \langle P_{\perp 2}\rangle]/2$ versus laboratory angle for α-α pairs in opposite side and same side configurations. Gating conditions are the same as those in Fig. 4.

Three separate multiplicity gates (high, low, and all) have been applied as described above. Prior to any interpretation let us note several trends for these Δ values: (a) They decrease with decreasing angle and become almost nil at 21° and 31° for beams of $(17-34)A$ MeV. (b) The high multiplicity and all multiplicity gates lead to almost the same Δ values. (c) The low multiplicity gate leads to higher Δ values, especially for the higher energies, $27A$ and $34A$ MeV. (d) For ring 4 ($\theta = 67°$) the Δ values are almost constant with changing incident energy.

Recall that Fig. 1–4 and Refs. [5] and [6] all present evidence for reaction class mixing for α's found at 21°, but also all present evidence for a conceptually simple mechanism for α-particle ejection at 67°. This process is evaporationlike emission from a group of composite nuclei formed by fusion (complete or incomplete) in central collisions [5,6,10,12]. The similar Δ values or recoil effects (for α pairs at 67°) seem to imply very similar masses for the composite nuclei formed in all of these ^{40}Ar reactions of 7 to $34A$ MeV. In this paper our first objective is to use these data at 67° to obtain the effective emitter masses.

Naturally we make model calculations for comparison to the data in order to seek quantitative estimates for these masses. For this purpose we first show results from a Monte Carlo program (KIN) written by making use of some subroutines from the simulation code MENEKA [13]. The logic of the program follows the usual steps for evaporative emission following fusion: (a) A projectile of mass A_p fuses with a target of mass A_t and the composite nucleus moves along the beam direction with velocity V_1^{ef} (see Fig. 5). (b) An α particle is emitted with velocity $V_{\alpha 1}$ (selected from an appropriate distribution) from an emitter of mass A_{em1} ($A_{em1} < A_p + A_t$). (c) A second α-particle is emitted with velocity $V_{\alpha 2}$ from an emitter of mass A_{em2} ($A_{em2} \leq A_{em1} - 4$) moving with velocity V_2^{ef}. Particle pairs are tested for geometrical and threshold acceptance, and then their characteristics are binned for comparison to the experimental data.

Our goal in these calculations is to vary the first emitter mass (A_{em1}) until we get the best fit to the data. Naturally, we wish to select the rest of the needed input so as to make the simulation as realistic as possible. For this purpose we use as much empirical information as possible: (a) We take account of incomplete fusion by reducing the effective projectile mass by the fractional LMT value, while retaining the beam velocity of ^{40}Ar. (b) We parametrize the intrinsic transverse momentum spectrum of the two α particles (both the same) by seeking a reasonable match to the observed spectra (averaged over all $\Delta\varphi$) using the functional form $P(\epsilon) \propto (\epsilon - V)^2 \exp(-\epsilon/T)$ for the center-of-mass energy distribution. The simulated (program KIN) and observed spectra for $\theta_{lab} \approx 67°$ are shown in Fig. 7. Note that an increase in the incident ^{40}Ar energy mainly increases the width of the α-particle spectrum (at 67°) rather than the magnitude of the average transverse momentum or energy. (More discussion of the role of this spectral width is given

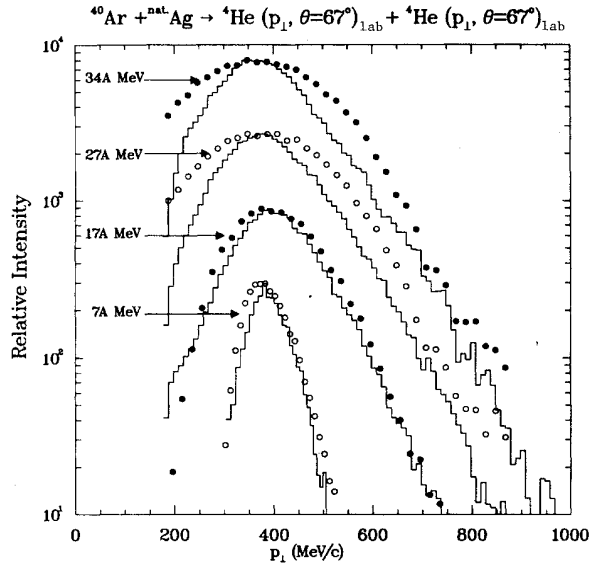

FIG. 7. Transverse momentum distributions for α particles detected in pairs at $\theta \approx 67°$ (all $\Delta\varphi$ values accepted). Histograms give the experimental data and points the simulated spectra (constrained to the same $\langle P_{\perp 1} \rangle$).

below.)

We have made a large number of simulation calculations to determine the dependence of the average value of Δ on the assumed emitter mass A_{em1}. It turns out that the sensitivity to A_{em2} and LMT are quite small for these reactions. This important fact allows us to focus the analysis on a determination of A_{em1}. Figure 8 shows calculated points from these simulations compared to horizontal bands that reflect the limits of the experimental error bars for the quantity Δ. One can obtain limits on the emitter masses from this analysis by reading off the mass values from the line intersections on Fig. 8.

In Fig. 9 we plot these deduced (first α) emitter masses versus ^{40}Ar beam energy. Also indicated are the average masses of the initial composite nuclei estimated from the fractional linear momentum transfer as discussed above. In the framework of incomplete fusion the decrease in emitter mass with beam energy has two aspects: (a) a decrease in LMT (or concomitant increase in total mass of the forward peaked particle spray) and (b) an increase in the average chain of evaporationlike particle emission prior to the detected α-α pair. By taking mass differences from Fig. 9 one can estimate the average evaporative mass loss prior to the emission of any pair of α particles. These average evaporative mass losses are 20 ± 10, 20 ± 10, 30 ± 10, and 20 ± 10 for $E/A = 7$, 17, 27, and 34 MeV, respectively. From calculations for evaporation after incomplete fusion we estimate quite comparable average evaporative mass losses before emission of randomly selected α pairs. (This is illustrated in Fig. 11 below.) Therefore, the notion of incomplete fusion and evaporationlike emission can account for these results quite well over the whole energy span of $(7-34)A$ MeV.

In another view one could conceive of highly dissipative collisions in which projectilelike and targetlike fragments maintain some sort of identity and emerge at small laboratory angles, i.e., deeply inelastic collisions with small scattering angle. Reexamination of Figs. 4 and 6 can give us some hints about emitters that are likely to be such targetlike fragments. The use of the low multiplicity gate emphasizes the role of such inelastic collisions compared to the most highly dissipative collisions. In

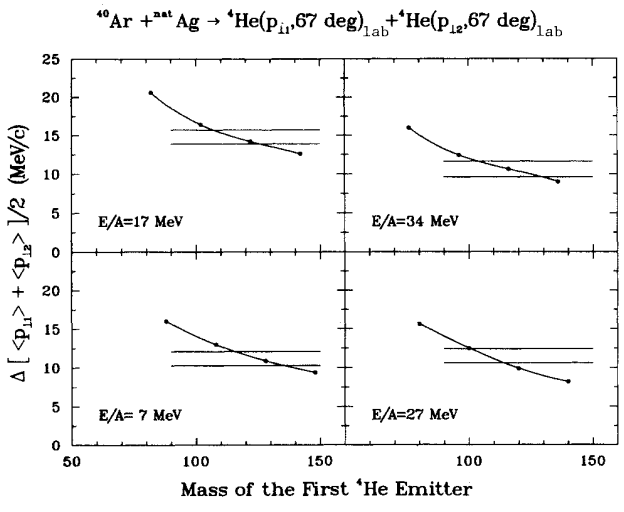

FIG. 8. Mean transverse momentum difference $\Delta = \Delta[\langle p_{\perp 1} \rangle + \langle P_{\perp 2} \rangle]/2$ versus mass of the first ^{4}He emitter for α-α pairs at $\theta_{lab} \approx 67°$. Horizontal bands give experimental upper and lower limits for one standard deviation. Points are calculated by simulations for successive α-particle emission; the lines are meant to guide the eye.

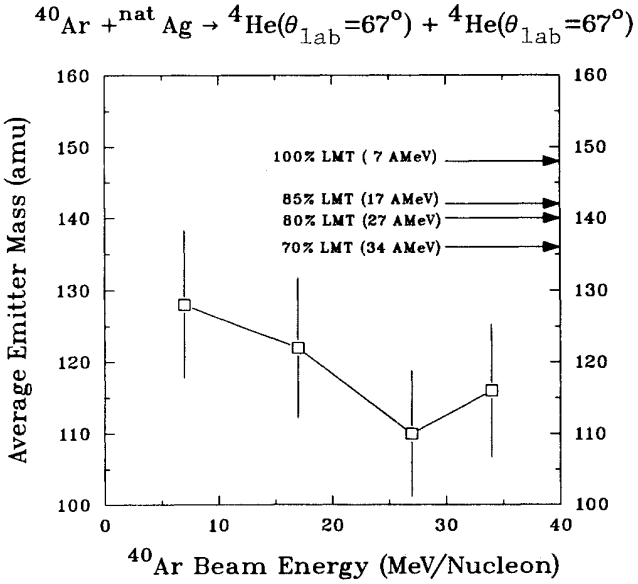

FIG. 9. Average emitter mass (prior to the emission of the first α in observed α-α pairs) obtained from Fig. 8 versus ^{40}Ar beam energy. The initial nuclear mass is indicated corresponding to the values taken for fractional linear momentum transfer, LMT.

Fig. 4 we see that the anisotropies (at $\theta_{lab}=67°$) are larger for the low multiplicity gate; this is expected for emitters with higher angular momenta or lower temperatures. In Fig. 6 we see that the Δ values are significantly larger for the low multiplicity gate; this is expected for emitters with smaller masses. These differences suggest that there is a distribution of emitters, and that the set with lowest multiplicity has lower excitation energy, smaller mass, and higher spin. This set of emitters (low multiplicity gate) is a relatively small part of the total analyzed; the total group (all multiplicity gate) is very similar to the emitter set at the other extreme (i.e., the high multiplicity gate).

There may, of course, be an admixture of impact processes, some better described by the phrase incomplete fusion (ICF) and some better described by the phrase deeply inelastic reactions (DIR). It is evident that the distinction between these classes could well be lost for the heavy excited nucleus, if the average fractional LMT diminishes for ICF and if the transferred mass increases for DIR. One normally thinks of deeply inelastic scattering with ejection of an observable projectilelike fragment, but a projectilelike fragment may well experience extensive breakup and excitation in a violent impact. Such collision violence could in the limit remove much of the distinguishability between DIR with its projectilelike fragment and ICF with its forward peaked spray of particles.

We have tried to extend this analysis to α-α pairs detected at smaller angles. The results (in a plot similar to Fig. 8) for angles of 21° and 31° yield no acceptable intersection between the data and the line from our calculations. There are a number of obvious problems. First, our analysis considers that the emission is from a rather heavy composite nuclear emitter that is moving relatively slowly. Hence the calculated transverse momentum shift from an α particle at $\theta\approx 21°$ is very small for a wide span of masses, and the quantity Δ loses its sensitivity. One could try a separate analysis for small angles that is based on α-particle emission from projectile fragments. Such an analysis could be interesting but is beyond the scope of this paper.

In Fig. 10 we show an extension of (or alternative to) this analysis for a variety of particle pairs (p and α detected at 67° and Li detected at 47°). Here our approach and our program are somewhat different from that discussed above. We did not seek to make fits to data with simulation calculations that employ different masses. Instead we have adopted the values of the average emitter mass as shown in Fig. 9, and in addition we have used the observed particle spectra as input (rather than an analytic generation function). Then we calculate relative energy shifts for same side versus opposite side configurations. For each particle pair, results from three simulations are shown: (a) the full line is for emission of each particle first in 50% of the pairs, (b) dashed line is for emission of the light particle first in 100% of the pairs, and (c) the dotted line is for emission of the heavy particle first in 100% of the pairs. Recall that the central collision group dominates production for all of these pairs, as shown by the multiplicity distributions [6].

Figure 10 is rather complex because it has several ob-

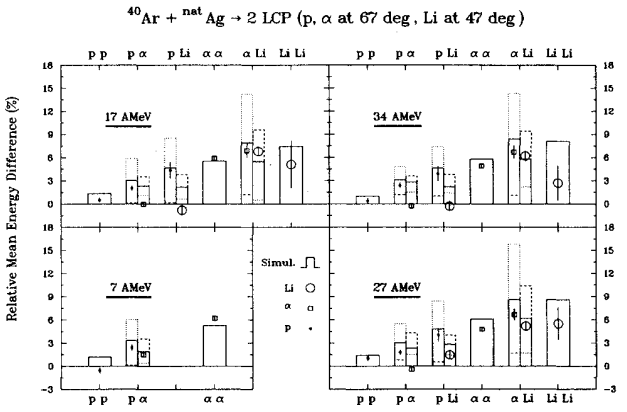

FIG. 10. Relative mean energy difference $\Delta\epsilon/\langle\epsilon\rangle$ for particles (p, α, and Li) detected in various pairs at $\approx 67°$ for p or α at $\approx 47°$ for Li. Points give the experimental data and histograms the simulated results. Emitter masses were taken from Fig. 9. Histograms with solid lines are for 50% first emission of each particle, those with dashed lines for 100% first emission of the lighter particle in the pair, and those with dotted lines for 100% first emission of the heavier particle.

jectives. First let us focus on the results for only the α-α pairs and compare them to those previously described. In these simulations we have adopted the average emitter mass values deduced previously and shown in Fig. 9. However, we have employed rather different program logic in that we pick α-particle energies directly from the observed spectra. This procedure gives, of course, a perfect fit to the data shown in Fig. 7. In spite of this alteration the calculated and observed energy shifts for α-α pairs in Fig. 10 remain essentially unchanged. Evidently the average energy shifts are not sensitive to the details of the spectral width, and depend mainly on the average emitter mass. Again with this program we have made tests for the dependence on input values of LMT used in the simulations. For these tests the individual emitter frame velocities (e.g., V_1^{ef}, $V_{\alpha 1}$ in Fig. 5) were changed substantially but the final laboratory velocities (e.g., $V_{\alpha 1}^{lab}$) were, of course, identical. These tests (e.g., for LMT of 60% and 80% for 34 A MeV ^{40}Ar) also resulted in negligible changes in the calculated energy shifts ($<0.3\%$ change for α-α pairs); hence the inferred average emitter mass is essentially independent of LMT.

A second objective of Fig. 10 is to test for a similar history in the formation of the other pairs of particles compared to the formation of α-α pairs as discussed above. Proton-proton pairs can be expected to experience very small shifts because the proton mass and momentum kick as so small. Indeed the experimental data for p-p pairs do show little or no shift from same to opposite side configurations. This comparison may seem trivial at first, but it gives strength to the basic assumption of right-left symmetry for the intrinsic particle emission. A reaction with nonzero directed transverse momentum or flow would violate this symmetry constraint [14].

The p-α pairs seem to be generally, but not completely, consistent with this picture of a recoiling composite nu-

cleus. Average proton energies are shifted by $\approx 2-3\,\%$ due to recoil from the α particles, consistent with proton emission prior to α emission for about half to three-quarters of the events. On the other hand, the energies of α particles (p-α pairs) experience little or no shift from the recoil due to proton emission. Interestingly, our prediction of a significant shift for the α particles in p-α pairs is not directly due to simple vector additions as displayed in Fig. 5. The simulation reveals a much more subtle effect related to the kinematic selectivity for coincident pairs. At first we suspected that the absence of this predicted shift in the experimental α spectra might be related to the presence of "kinematic noise" or random jitters in $V_1^{\rm ef}$ or $V_2^{\rm ef}$ (see Fig. 5) that overwhelm the small proton recoil kicks [7]. This effect has also been studied via simulations for multibody emission scenarios, but at present we cannot account for the very small shifts observed for the α's from p-α pairs at $17A$, $27A$, and $34A$ MeV.

The α-Li as well as p-Li cases in Fig. 10 are of particular interest because Li fragments are candidates for the proposed "instantaneous" multifragmentation process. For the α-Li (p-Li) coincidences the α's (p's) are shifted by 6–8 % (3–5 %). These shifts are predicted for α or p emission prior to Li emission in about 50% of the reactions. Shifts in the Li energies are also roughly consistent with the calculations for α-Li and Li-Li pairs, but are apparently too small for p-Li pairs. Nevertheless the major point is that the energy shifts for α particles (or protons) in α-Li (p-Li) pairs do suggest α particle (or p) emission prior to the Li fragments in $\approx 50\%$ of the events. This would seem to argue against any especially rapid mechanism for Li ejection compared to that for the copiously evaporated ^{1}H and ^{4}He particles. Recall that the simulation calculations shown in Fig. 10 were made for only two emission steps. The assumption has been made that the emission of additional particles does not affect the average shifts in momentum or energy. Results from multibody emission calculations are also consistent with this assumption as described below.

From the discussion above it seems that the overall pattern of the data can be described by incomplete fusion in association with statistical emission of protons, α particles and even Li fragments. Therefore, we have made multistep statistical model calculations using the code MODGAN [13]. Results from such calculations are shown in Fig. 11, which uses the same format as Fig. 10. The major difference is that the MODGAN calculation follows a multistep emission cascade which generates the emitter masses at each step. Therefore, the average emitter mass is a natural result rather than an input quantity. The results of this multistep calculation (Fig. 11) account very well for the energy shifts for α-α coincidences; this indicates a consistency with the two-step calculations that led to the masses shown in Fig. 9. In addition the calculated results for p-p and p-α pairs are essentially the same (in Figs. 10 and 11) for the two-step and multistep approaches. Data for the p-p pairs agree quite well with the model. However, the observed energy shifts are again smaller than those calculated for α's in the p-α pairs. Note that the energy shifts for Li-Li pairs are better described in Fig. 11 by the statistical-model emission chains than they were in Fig. 10. There is a selection by this model of higher values of the emitter mass ($A_{\rm eml}$) for Li-Li pairs than for α-α pairs. In Fig. 10 the same values of $A_{\rm eml}$ were used for all pairs, and this led to larger calculated Li energy shifts.

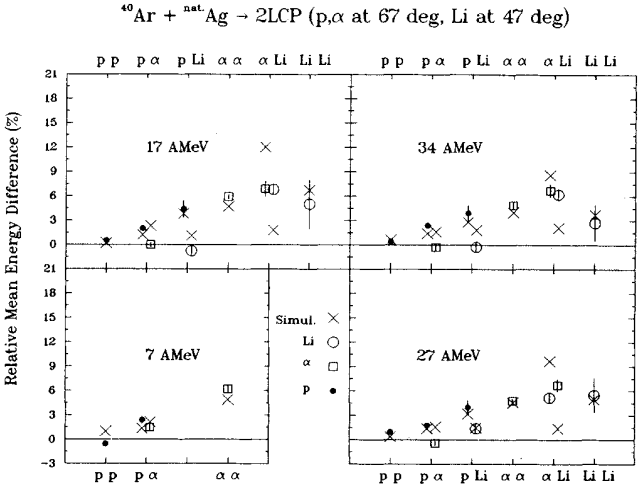

FIG. 11. Relative mean energy difference $\Delta\epsilon/\langle\epsilon\rangle$ just as in Fig. 10. Here the calculated values are shown as crosses. They result from multistep emission calculations that begin with incomplete fusion (LMT values as for Fig. 1), followed by a Monte Carlo statistical-model description of the deexcitation chains (MODGAN, Ref. [13]). The parameter "a" was chosen as $A/10$ MeV^{-1} for $(7-27)A$ MeV and $A/15$ MeV^{-1}) for $34A$ MeV; this gave energy spectra which compare well to the data. Spin zones were taken from Ref. [5].

The statistical model calculations are quite interesting for the Li-p and Li-α pairs. Results in Fig. 11 (in contrast to Fig. 10) are completely acceptable for the Li-p pairs, but for Li-α pairs there are almost identical deviations for each incident ^{40}Ar energy. The statistical model predicts smaller (larger) Li (p and α) energy shifts, because Li emission precedes both p and α emission in about $\frac{2}{3}$ of the calculated pairs. The data agree with these predictions for Li-p, but seem to indicate a lower preference for initial emission of Li in Li-α pairs. This result is interesting and suggestive; it merits further study in future work.

The major conclusion from Figs. 10 and 11 is that small but clear recoil shifts are observed for essentially all particle pairs from these ^{40}Ar+Ag reactions. The magnitude of these shifts is generally consistent with sequential particle ejection from a group of composite nuclei formed by incomplete fusion reactions. Some subtleties remain in the smaller than expected shifts for α particles in p-α pairs, and for both fragments in α-Li pairs. Analysis and calculations have been initiated on a new set of measurements that employ detectors with much smaller angular acceptance.

The average effective masses that we infer for the heavy excited composite nuclei vary from ≈ 130 to 110 for ^{40}Ar beams of $7A$ to $34A$ MeV. These values are con-

sistent with incomplete fusion but could allow an admixture of mechanisms with resemblance to both incomplete fusion and deeply inelastic collisions. However, the distinction between these designations is essentially lost for the lower fractional linear momentum transfers in ICF or the large mass transfers in DIR that seem to characterize these reactions of Ar+Ag at ≈ 30 MeV per nucleon.

Financial support has been provided by the United States Department of Energy and the Centre National de la Recherche Scientifique (France). Time and support from the Cornell National Supercomputer Facility is also appreciated. T.E. is also grateful to the Société Lyonnaise de Banque for partial support. We thank R. A. Lacey for many helpful ideas and discussions.

[1] B. B. Back, K. L. Wolf, A. C. Mignerey, C. K. Gelbke, T. C. Awes, H. Breuer, V. E. Viola, and P. Dyer, Phys. Rev. C **22**, 1927 (1980).

[2] E. Suraud, C. Grégoire, and B. Tamain, Prog. Nucl. Part. Sci. **23**, 357 (1989), and references therein.

[3] D. H. Boal, C. K. Gelbke, and B. K. Jennings, Rev. Mod. Phys. **62**, 553 (1990), and references therein.

[4] D. Drain, A. Giorni, D. Hilscher, C. Ristori, J. Alarja, G. Barbier, R. Bertholet, R. Billery, B. Chambon, B. Cheynis, J. Crancon, A. Dauchy, P. Désequelles, A. Fontenille, L. Guyon, D. Heuer, A. Lleres, M. Maurel, E. Monnand, C. Morand, H. Nifenecker, C. Pastor, J. Pouxe, H. Rossner, J. Saint-Martin, F. Schussler, P. Stassi, M. Tournier, and J. B. Viano, Nucl. Instrum. Methods Phys. Res. Sec. A **281**, 528 (1989).

[5] T. Ethvignot, A. Elmaani, N. N. Ajitanand, J. M. Alexander, E. Bauge, P. Bier, L. Kowalski, M. T. Magda, P. Désequelles, H. Elhage, A. Giorni, D. Heuer, S. Kox, A. Lleres, F. Merchez, C. Morand, D. Rebreyend, P. Stassi, J. B. Viano, F. Benrachi, B. Chambon, B. Cheynis, D. Drain, and C. Pastor, Phys. Rev. C **43**, R2035 (1991).

[6] M. T. Magda, T. Ethvignot, A. Elmaani, J. M. Alexander, P. Désesquelles, H. Elhage, A. Giorni, D. Heuer, S. Kox, A. Lleres, F. Merchez, C. Morand, D. Rebreyend, P. Stassi, J. B. Viano, F. Benrachi, B. Chambon, B. Cheynis, D. Drain, and C. Pastor, Phys. Rev. C **45**, 1209 (1992).

[7] T. Ethvignot, N. N. Ajitanand, C. J. Gelderloos, J. M. Alexander, E. Bauge, A. Elmaani, R. A. Lacey, P. Désequelles, H. Elhage, A. Giorni, D. Heuer, S. Kox, A. Lleres, F. Merchez, C. Morand, D. Rebreyend, P. Stassi, J. B. Viano, F. Benrachi, B. Chambon, B. Cheynis, D. Drain, and C. Pastor, Nucl. Phys. **A545**, 347c (1992).

[8] W. G. Lynch, L. W. Richardson, M. B. Tsang, R. E. Ellis, C. K. Gelbke, and R. E. Warner, Phys. Lett. **108B**, 274 (1982).

[9] R. Lacey, N. N. Ajitanand, J. M. Alexander, D. M. de Castro Rizzo, G. F. Peaslee, L. C. Vaz, M. Kaplan, M. Kildir, G. La Rana, D. J. Moses, W. E. Parker, D. Logan, M. S. Zisman, P. DeYoung, and L. Kowalski, Phys. Rev. C **37**, 2561 (1988).

[10] C. J. Gelderloos, J. M. Alexander, J. Boger, P. DeYoung, A. Elmaani, M. T. Magda, A. Narayanan, and J. Sararfa (unpublished).

[11] V. Viola, Nucl. Phys. **A502**, 531c (1989); D. Jacquet *et al.*, *ibid.* **A509**, 195 (1990); A. Lleres, Ph.D. thesis, Institut des Sciences Nucléaires de Grenoble, 1988, and references therein.

[12] A. Elmaani, N. N. Ajitanand, J. M. Alexander, R. Lacey, S. Kox, E. Liatard, F. Merchez, T. Motobayashi, B. Noren, C. Perrin, D. Rebreyend, Tsan Ung Chan, G. Auger, and S. Groult, Phys. Rev. C **43**, R2474 (1991).

[13] A. Elmaani, N. N. Ajitanand, T. Ethvignot, and J. M. Alexander, Nucl. Instrum. Methods Phys. Res. **A313**, 401 (1992). This paper describes two simulation programs (MENEKA and COULGAN) that use three-body trajectories. The multistep statistical-model code MODGAN (N. N. Ajitanand and J. M. Alexander, unpublished) has also been used in conjuction with the above codes to help elucidate certain effects of complex emission chains [5,11].

[14] W. K. Wilson, D. Cebra, S. Howden, J. Karn, D. Krofcheck, R. Lacey, T. Li, A. Nadasen, T. Reposeur, A. Vander Molen, C. A. Ogilvie, G. D. Westfall, and J. S. Winfield, in *Seventh Winter Workshop on Nuclear Dynamics,* edited by W. Bauer and J. Kapusta (World Scientific, Singapore, 1991), p. 139.